J Oceanogr
DOI 10.1007/s10872-017-0427-z

ORIGINAL ARTICLE

Using major nutrient concentrations to derive vertical movement of water masses in the coastal region of eastern Taiwan

Su-Cheng Pai[1] · Sen Jan[1] · Tung-Yuan Ho[1,2] · Jin-Yuan Liu[3] · Ken-Sheng Chu[1,2] · Wen-Huei Lee[1] · Cheng-Yun Wang[1] · Ping-Yi Huang[4] · Hung-Yu Hsu[4] · Yiing-Jang Yang[1]

Received: 9 July 2016 / Revised: 16 April 2017 / Accepted: 17 April 2017

Abstract Significant variations of phosphate and silicate concentrations have been observed in seawater from selected industrial pipelines at intake depths between 400 and 710 m off the Hualien coast, eastern Taiwan, revealing a strong vertical movement of water mass in this intermediate layer. An intensive monitoring experiment was carried out, in which pipeline seawater from three land-based pumping stations and seawater collected by a research vessel were obtained and analyzed in parallel during a 2-day observation period. The results showed clearly that the changes of nutrient concentrations in both pipeline and shipboard samples followed a semidiurnal cycle. The maximum vertical displacement occurred in the 300–800 m layer with a scale as surprisingly large as 100 m, when compared with that observed in other areas. The tidal cycles for different layers may not synchronize with surface tide or each other. Empirical equations have been implemented between nutrient concentrations and temperature for the Hualien off-shore area. The equation can be used to check temperature variation of the intermediate water by measuring either phosphate or silicate in pipeline seawater.

Keywords Pipeline · Intermediate water · Phosphate · Silicate · Temperature · Internal wave

1 Introduction

Deep ocean water (defined here as seawater below the euphotic zone at a depth of more than ca. 200 m) is an important resource in eastern Taiwan (Takahashi et al. 2012; Pai et al. 2015). At present, five pipelines have already been deployed by three local factories along the Hualien coast (Fig. 1; Table 1), and the cold deep ocean water is used for mariculture and production of drinking water. The collecting depths are at 618, 662, and 710 m for the three main pipelines with two supplemental ones at 400 and 430 m, respectively. At the far end of each pipeline there is a supporting rack to raise the pipe head a few meters above the ocean floor to prevent it from taking up bottom suspension. Intuitively, the water mass at such a depth should be temporally stable, clean, cold, and rich in micronutrients. However, according to the operational records at three factories the water temperature might go up and down from time to time, and the daily variation could be as large as a few degrees (°C). The scale of this variation is significant enough to be concerned about in further application such as thermo-control for algae growth. It should be noted that without a sensor installed at the intake point, the actual temperature change at the intake point is still uncertain. Nonetheless, the information has already reflected that the deep ocean water mass might not be as static as it was thought previously. This interesting phenomenon has yet to be reported in the Hualien area and the reasons need to be clarified.

Several recent reports on physical oceanography might provide a clue: The variation of temperature could be direct

Deceased: Wen-Huei Lee.

✉ Yiing-Jang Yang
yjyang67@ntu.edu.tw

[1] Institute of Oceanography, National Taiwan University, Taipei, Taiwan

[2] Research Center for Environmental Changes, Academia Sinica, Taipei, Taiwan

[3] Institute of Undersea Technology, National Sun Yat-sen University, Kaohsiung, Taiwan

[4] Water Resources Division, Stone and Resource Industry R&D Center, Hualien, Taiwan

Published online: 28 April 2017

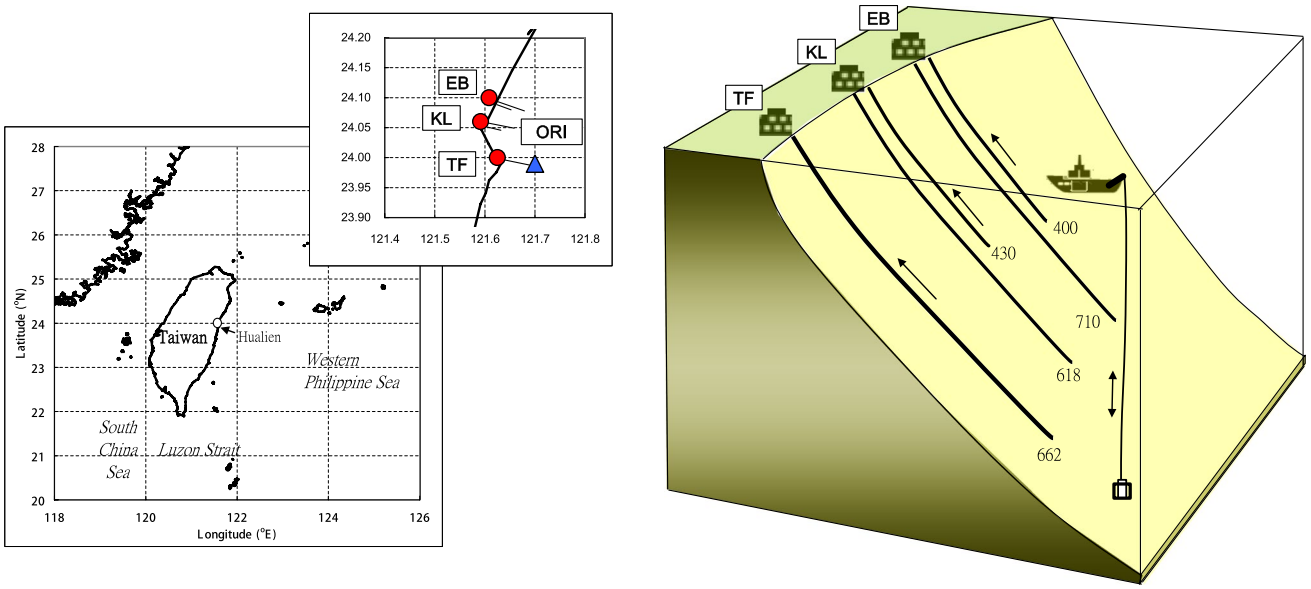

Fig. 1 Location of deep ocean water pipelines deployed off Hualien coast, eastern Taiwan. They are operated by three factories (TF, KL, and EB). The intake points are at the far end of pipelines at depths between 400 and 710 m (also see Table 1). In this study the off-shore water column samples were collected by a research vessel (R/V Ocean Researcher I, Cruise 1123) which was anchored near the intake site of TF-662

Table 1 Industrial pipelines deployed off Hualien coast, eastern Taiwan

Code	Intake depth (m)	Pipe length (m)	Pipe i.d. (cm)	Max intake vol (m^3 day^{-1})	Max flow speed (ms^{-1})*	Min delivery time (h)*
EB	710	4200	15.5	800	0.49	2.4
EB	400	2300	15.5	800	0.49	1.3
KL	618#	2900	15.5	980	0.60	1.3
KL	430*	2000	15.5	980	0.60	0.9
TF	662	4300	25.5	2400	0.54	2.2

EB Eastlife Biotech Co., *KL* Kuang-Long Biotech Co., *TF* Taiwan Fertilizer Co.

* Estimated values

\# Not included in this study

or indirect results of internal tidal waves that are transmitted either from the Luzon Strait in southern Taiwan (Lien et al. 2005, 2013; Alford et al. 2011, 2015) or from the southern flank of the Ilan Ridge between Ryukyu and Taiwan (Lien et al. 2014). The generation force is related to the barotropic tide of the Pacific Basin which flows over submarine ridges and produces a vertical displacement of up to 150 m in the upper ocean (Niwa and Hibiya 2004; Jan et al. 2007, 2008). With these in mind we need first to collect enough data to confirm the existence of internal waves off the Hualien area, and then to link them with the observed temperature variations found in the pipeline water.

An indirect chemical method has been proposed to estimate the temperature at the pipeline's far end (Pai et al. 2015) by measuring silicate in the pipeline water. Silicate has a close relationship with temperature along the water column and its concentration will not change during the pumping process. Following this thought, we have decided to monitor silicate regularly at selected land based pumping stations to see if the concentration also varies like temperature does. Phosphate was also measured in parallel not only as a double check but also due to the practical reason that silicate measurements need to be corrected for phosphate interference. In order to calibrate the relationship between these nutrients and temperature, we have used a research vessel to collect off-shore water and compare the results almost simultaneously with that of the pipeline water.

2 Materials and methods

Both phosphate and silicate in pipeline seawater were measured colorimetrically. Phosphate reacts with molybdate reagent under an acidic condition to form a phosphomolybdenum complex which is further reduced by ascorbic acid to form a dense blue complex. The final color is measured at 880 nm (Pai et al. 1990). Silicate also reacts with molybdate to form a yellowish silicomolybdenum complex. The color is measured directly at 400 nm, but the result needs a correction as phosphate interferes at this wavelength by producing a similar absorptivity equivalent to half of that of the silicate color (Ting 2009). A simple correction process was made by:

$$[\mathrm{Si}]_{\mathrm{corr}} = [\mathrm{Si}]_{\mathrm{raw}} - 0.5[\mathrm{P}] \quad (1)$$

where $[\mathrm{Si}]_{\mathrm{corr}}$ and $[\mathrm{Si}]_{\mathrm{raw}}$ are the corrected and raw Si concentrations (μM), [P] the measured phosphate concentration (μM). In this study, since [P] was much less than [Si] (the ratio was between 0.02 and 0.04), the correction term made for raw silicate data was between 1 and 2%.

Sample storage: Samples were filled in 500 mL PET bottles, sealed and then wrapped in opaque bags and stored in boxes to shade completely from light. Since the analyses were made batch-wise, the storage effect was carefully checked. In a prior test, we have found that clear samples (with turbidity less than 1 NTU) can be stored for up to 4 months at room temperature without noticeable change in nutrients.

3 Results and discussion

3.1 Experiment 1: long-time observation

The first observation program was carried out at two pipeline pumping stations, i.e., TF-662 and KL-430. Samples were collected by the staff of the factories on a daily basis except for weekends and holidays. Thus, 15 bottles were collected at TF-662 between Jan 7–13 and March 24–31, 2015, whereas 48 bottles were obtained at KL-430 between Jan 8-May 1, 2015, covering a 4-month period. The whole batch of the stored samples was measured a week after the last sampling date.

The results are shown in Table 2 and Fig. 2 in which nutrient concentrations were plotted following a sampling sequence. Basically, the data points give average concentration zones but are randomly distributed within the ±2σ range. At TF-662, the phosphate concentrations ranged from 2.28 to 2.62 μM, with a mean value of 2.48 ± 0.08 μM (r.s.d. = ± 3.1%, n = 15), whereas the silicate concentrations ranged from 75.9 to 85.6 μM, with a mean value of 82.1 ± 3.3 μM (r.s.d. = ±4.1%, n = 15). At KL-430, the range for phosphate was found to be 1.23–1.93 μM, with a mean value of 1.60 ± 0.19 μM (r.s.d. = ± 11.7%, n = 48);

Table 2 Daily variations of phosphate and silicate at KL-430 and TF-662

Phosphate (μM)					Silicate (μM)				
Max	Min	Mean	Std. dev.	R.s.d. (%)	Max	Min	Mean	Std. dev.	R.s.d. (%)
KL-430 (Jan 8–May 1, n=48)									
1.93	1.23	1.6	0.19	11.7	55.8	30.6	42.3	7.0	16.6
TF-662 (Jan 7-Jan 13; Mar 25-31, n=14)									
2.62	2.28	2.47	0.08	3.2	85.6	75.9	82.1	3.3	4.1

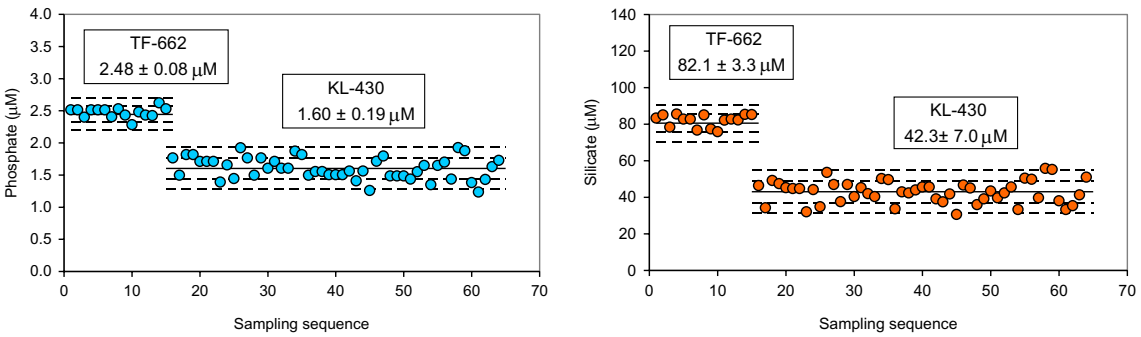

Fig. 2 Variations of phosphate and silicate concentrations at two pipeline pumping stations. Samples were generally collected on a daily basis. Fifteen bottles were obtained at TF-662 between Jan 8 and Mar 31, 2015, whereas 48 bottles at KL-430 between Jan 8 and May 1, 2015. *Solid lines* indicate the mean values and *dashed lines* mark ±1σ and ±2σ levels

the range for silicate was 30.6–55.8 μM, with a mean value of 42.3 ± 7.0 μM (r.s.d. = ± 16.6%, $n = 48$). The patterns of the two parameters are parallel, but the relative variations for silicate were slightly larger than those for phosphate. The relative variations at the shallower KL-430 were larger than that at the deeper TF-662.

3.2 Experiment 2: short-time observation

On April 20, 2015, after an earthquake (No.22, 9:42 AM, magnitude 6.4, epicenter 30.2 km deep, 83.6 km east of Hualien. Source: Taiwan Central Weather Bureau), we asked the staff of the three factories to help collect pipeline water starting from 9:00 on an hourly basis. A total of 18 samples were obtained on that day, and they were delivered to the laboratory in Taipei and analyzed the next day. The data are shown in Fig. 3. No earthquake-induced turbidity signals were found. Instead, hourly variations of nutrients did exist and the changes could be very drastic within 1 h. At EB-710, the mean concentrations were [P] = 2.64 ± 0.09 μM, [Si] = 91.1 ± 4.4 μM; at KL-430, [P] = 1.61 ± 0.09 μM, [Si] = 45.0 ± 2.9 μM; at TF-662, [P] = 2.37 ± 0.18 μM, [Si] = 76.9 ± 7.0 μM. These ranges are quite similar to those of the long-term observation. However, the variation patterns for the three layers are obviously not synchronized. There might be two reasons: (i) the time lag due to different pipeline lengths or/and (ii) the phase lags at different depths. The former can be estimated by calculating the pipeline lengths and velocities derived from pumping rates (Table 1). The latter would need a further verification by off-shore CTD measurements.

3.3 Verdict of vertical displacement

A review of historical hydrographic data east of Hualien (Chen 2005; Jan et al. 2015) shows that the surface mixing layer is less than 100 m thick. It is deficient in phosphate (<0.1 μM) and low in silicate (<3 μM). Below this layer both nutrient concentrations increase with depth to a maximum at 1100 m for phosphate and 2600 m for silicate. The average slopes of the profiles, i.e., d[P]/dz and d[Si]/dz at the designated depths (430, 662, and 710 m) can be obtained graphically. If the nutrient variation is a regular movement, the maximum vertical displacement Δz can be estimated statistically by taking a fourfold standard deviation value ($4\sigma_P$ or $4\sigma_{Si}$, at 95% confidence level) and divided by the profile slope d[C]/dz:

$$\Delta z\ (\mathrm{m}) \fallingdotseq 4\sigma / (\mathrm{d[C]/d}z) \tag{2}$$

In Table 3, using phosphate data, the possible maximum vertical displacements Δz were estimated to be 161, 126, and 104 m at depths of 430, 662, and 710 m, respectively, whereas similar displacements of 171, 107, and 102 m were obtained using silicate data. If these verdicts

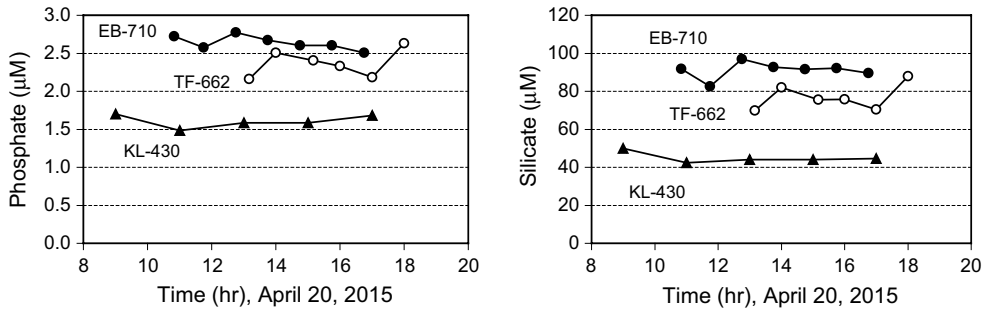

Fig. 3 Variations of phosphate and silicate concentrations in pipeline waters collected at three different factories (marked with intake depths) as EB-710, TF-662, and KL-430. Sampling was made on April 20, 2015, from 9:00 to 18:00. No direct correlation was found between the three pipelines, but the changes for P and Si concentrations were apparently parallel

Table 3 Verdict of vertical displacement by taking account of variations of nutrients

Depth (m)	No. of data	Phosphate (μM)		Slope d[P]/dz	Δz (m)	Silicate (μM)		Slope d[Si]/dz	Δz (m)
		mean	σ			mean	σ		
430	55	1.60	0.16	0.0040	161	43.1	5.9	0.138	171
662	21	2.45	0.12	0.0038	126	80.6	5.1	0.190	107
710	7	2.64	0.09	0.0035	104	91.1	4.4	0.173	102

Vertical displacement $\Delta z = 4\sigma$/slope

were correct, then an oscillation movement would be expected to occur in the intermediate layer (between 400 and 700 m or 10–6 °C) with an amplitude exceeding 100 m, a scale that may be larger than one can imagine in such a deep layer.

3.4 Experiment 3: intensive monitoring

A united "land-sea" intensive monitoring experiment was carried out during Nov. 3–5, 2015. Participants were split into two groups: the "land" group collected pipeline water at three factories every hour for more than 24 h. The "sea" group were onboard a research vessel (Ocean Researcher I, Cruise 1123, from Kaohsiung to Hualien, Nov. 2–5, 2015) to operate CTD repeatedly and collect water samples by an attached rosette sampler. The ship was stopped at 23°59′00″ N, 121°42′00″ E (bottom depth ca. 950 m), ca. 4 km from the coast, near the TF-662 intake site. During the 24-h period (starting 17:00 pm, Nov. 4), the CTD unit was deployed 19 times, and water samples were collected in 11 up-casts using 10-L X-Niskin bottles mounted on the rosette sampler. The sampling depths were set at 50, 100, 150, 200, 300, 400, 500, 600, and 700 m, with a final depth at 10 m above the bottom (ca. 950 m). Surface seawater was obtained by a dipping pump immersed into the water at 5 m depth. All samples were filled directly into 500 mL PET bottles, covered with blankets, and stored at room temperature. After the ship docked at Hualien Port on Nov. 5, all samples, together with the "land" samples, were delivered promptly to the laboratory in Taipei. The analyses of nutrients were completed within the next 48 h.

3.4.1 Land group data

The land group sampling was carried out separately every hour at the three factories. The starting times and numbers of samples collected were: KL-430: from 16:00, Nov. 3, 26 bottles; EB-400: from 08:30, Nov. 4, 34 bottles; TF-662: from 08:00, Nov. 4, 34 bottles. The total time span covered 50 h. The sampling at KL-430 was earlier, but had a 10-h overlapping period with later started samplings at EB-400 and TF-662. Results are plotted against time lapse as shown in Fig. 4. The surface tide record at Hualien Station (Source: Taiwan Central Weather Bureau) is also presented. In order to identify the relationship between nutrient concentration variations and the tidal cycle, an autocorrelation analysis was made on each set of data containing N pair numbers (X_1, Y_1,…, X_N,Y_N). The autocorrelation function at a given lag number k, ACF (k), was calculated by:

$$\mathrm{ACF}(k) = \frac{\sum_{i=1}^{N-k} (Y_i - \overline{Y})(Y_{i+k} - \overline{Y})}{\sum_{i=1}^{N} (Y_i - \overline{Y})^2} \quad (3)$$

where $\overline{Y}$ is the mean value and each lag is 1 h. The resultant correlograms are also shown in Fig. 4. All diagrams show an obvious semidiurnal tidal pattern with two highs and two lows in 25 h.

The nutrient concentration ranges at KL-430 and EB-400 are almost the same, and the patterns are likely connectable. The range for phosphate concentration at KL-430 was 1.45–2.00 μM, the mean value was 1.69 ± 0.15 μM (n = 26), whereas at EB-400 the range was 1.35–1.80 μM and the mean value was 1.64 ± 0.11 μM (n = 34). The silicate concentration at KL-430 was 32.6–43.3 μM with a mean value of 39.9 ± 4.6 μM (n = 26), whereas at EB-400 the range was 30.8–48.2 μM with a mean value of 39.1 ± 4.7 μM (n = 34).

As to the deeper water at TF-662, the phosphate concentration ranged from 2.05 to 2.50 μM and the mean value was 2.35 ± 0.08 μM (n = 34), whereas the silicate concentration ranged from 60.9 to 95.3 μM and the mean value was 82.1 ± 6.7 μM. These values are quite similar to previous data as shown in Figs. 2 and 3.

3.4.2 Shipboard CTD data

The composite profiles of temperature and salinity (19 casts) are shown in Fig. 5, and the T-S diagram in Fig. 6. It can be seen that the mixed layer (T around 26 °C) is about 50 m thick, and a salinity maximum of 34.8 is found at 80 m or 20 °C. Below this depth both temperature and salinity profiles become scattered, but on the T-S diagram all lines merge together below 20 °C, indicating vertical rather than horizontal movements predominate.

There are two dashed lines in Fig. 6 showing the envelope of T-S data for the eastern Taiwan area. The envelope is composed by two major water column types, the West Philippine Sea type (WPS) and the South China Sea type (Pai et al. 2015). The intermediate layer can be defined graphically by the two intersects of the two types at 15 and 2 °C, respectively. The water mass east of Taiwan can be considered as the result of the isopycnal mixing of the two major water columns. Below 20 and above 8 °C, the water resembles more WPS than SCS type, whereas below 8 and above 4 °C, the influences from both water column types are nearly equal. The details about the spatial and temporal variations and the exchange of the two water types are referenced in Mensah et al. (2014, 2015), which delineate the variability and evolution of the tropical and intermediate waters east of Taiwan.

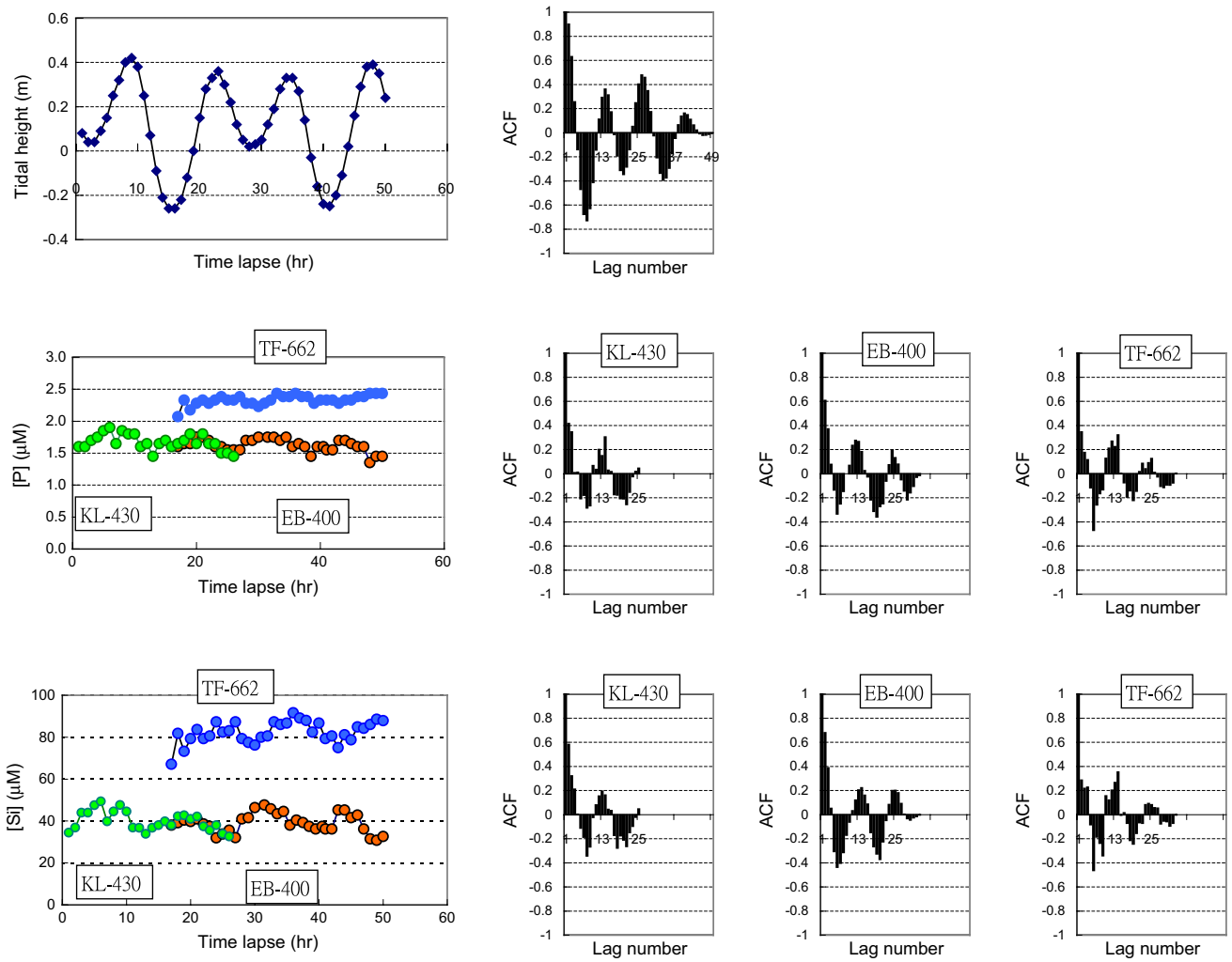

Fig. 4 Time series plots and autocorrelation plots of (*top*) tidal height at Hualien (*middle*) phosphate and (*bottom*) silicate at three pipeline stations marked with their intake depths, i.e., KL-430, EB-400, and TF-662. The *horizontal scale* shown is the time lapse in hour-long increments beginning at 15:00, Nov 3, 2015. The correlograms are shown on the *right* starting from the first samples

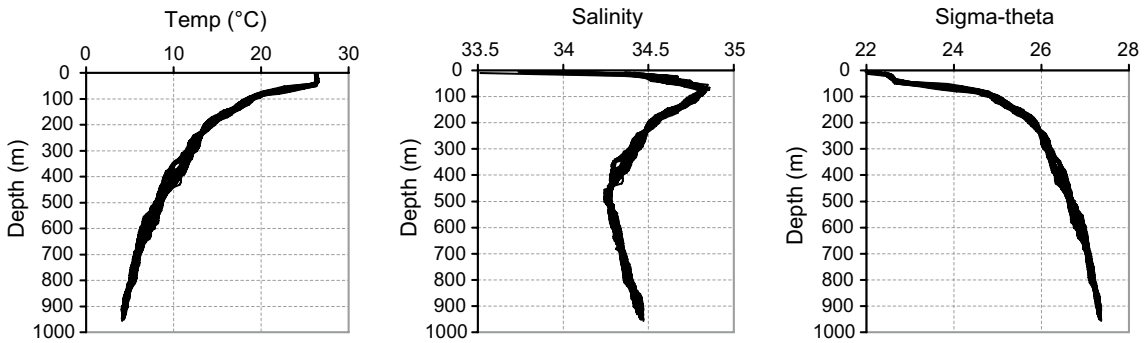

Fig. 5 Composite profiles of temperature, salinity, and sigma-theta of 19 CTD casts (in 24 h) at the anchored station, 4 km off the Hualien coast

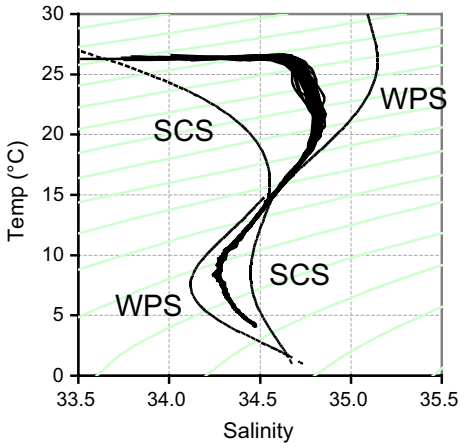

Fig. 6 T-S diagram showing the characteristics of the water column off Hualien coast as a hybrid of the West Philippine Sea type (WPS) and the South China Sea type (SCS). Below 25 °C and above 8 °C the water column has more WPS type properties. Below 8 °C and above 4 °C the influences from both types are nearly equal

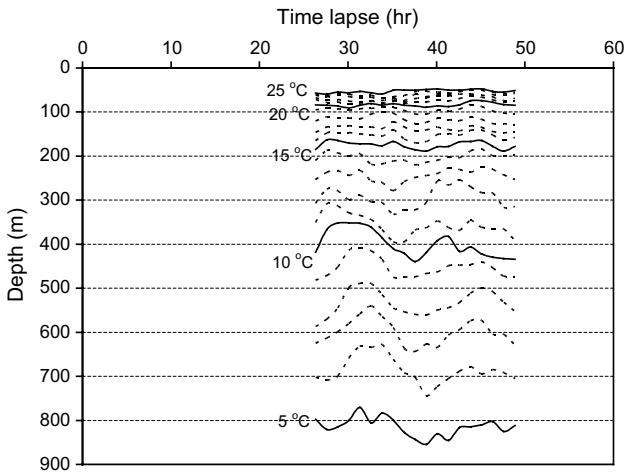

Fig. 7 Vertical semidiurnal displacements as shown by temporal variation of isothermal lines between 25 and 5 °C. During the observed 24-h period, vertical displacements of ca. 100 m occurred below 12 °C (corresponding to deeper than 300 m layers). The time scale is the same as Fig. 4

The variations of isothermal depths from 19 CTD casts are plotted in Fig. 7. The standard deviation of depth of a given isothermal line is noted as σ_d, which is used to estimate the average vertical displacement by $\Delta z = 4\ \sigma_d$. In Table 4 it can be seen that above 20 °C or ca. 100 m the vertical displacement was almost unnoticeable (<20 m). Below this depth it increased gradually to 93 m at 12 °C (or ca. 300 m). The oscillating amplitude maintained at almost the same scale (84–124 m) all the way down to the bottom.

3.4.3 Shipboard nutrient data

Vertical profiles of phosphate and silicate from 11 rosette casts are plotted in Fig. 8. Temporal variations of nutrient concentrations at fixed depths are shown in Fig. 9. The verdicts on vertical variations are overlaid for comparison. The surface mixing layer is ca. 50 m thick, in which the phosphate concentration is less than 0.05 μM, whereas the silicate concentration is about 1 μM. Both nutrients increase with depth. At 950 m the average concentration for phosphate and silicate are ca. 2.7 and 110 μM, respectively. The largest variations of nutrient concentrations indeed occurred in the intermediate layers, as has been indicated in Fig. 7.

3.4.4 Vertical displacement

A quantitative comparison was made on vertical displacement between CTD measurements and that estimated by chemical methods (see Table 4).

The chemical methods include (i) by analyzing nutrient variations in pipeline water and (ii) by analyzing nutrient variations in shipboard collected seawater. The vertical displacement was estimated by Δz (m) ≒ 4 σ/(d[C]/dz) (Eq. (2)). For pipeline waters the calculated results were between 86 and 128 m. For shipboard collected waters the results were between 76 and 122 m. These ranges match perfectly with that obtained by CTD measurements and also those verdict values shown in Table 3. It is reasonable to conclude that the vertical displacements are around 100 m for depths from below 300 m down to near the bottom.

3.4.5 Period and phase lag

It should be noted that even all diagrams in Fig. 4 show obvious semidiurnal cycles; they are not synchronized. To illustrate the phase differences, a central running mean process ($n = 5$) was made on chemical data to give a filtered sinusoidal-like curve:

$$\mathrm{C}_{\mathrm{mean}}(t) = \frac{C_{t-2} + C_{t-1} + C_t + C_{t+1} + C_{t+2}}{5} \tag{4}$$

The curve gives obvious crests and valleys, and the time span between each pair of crests and valleys can be estimated graphically (Fig. 10). Although the method is quite primitive, it is useful to estimate the time span between peaks and valleys. In Fig. 10a the average period for the surface tidal height is 12.9 ± 0.9 h ($n = 6$), matching the semidiurnal M2 tidal cycle ($T = 12.42$ h).

In Fig. 10b, the variation curves of silicate concentration in pipelines KL-430/EB-400 also show semidiurnal cycles (primarily M2) but the phase is likely 2 h ahead of

Table 4 Estimation of vertical displacements by CTD measurements and nutrient analyses

Method	Temp (°C)	Max (m)	Min (m)	Diff (m)	Mean (m)	$\pm\sigma_d$ (m)	n	Δz (m) estimated
Shipboard CTD	25	59	47	12	52	3.9	19	15
Depth of isothermal lines	20	91	74	17	84	4.5	19	18
	15	189	163	26	175	8.3	19	33
	14	220	184	36	203	11.0	19	44
	13	279	225	54	244	13.7	19	55
	12	332	254	78	294	23.2	19	93
	11	395	308	87	357	24.3	19	97
	10	440	352	88	400	30.6	19	122
	9	482	410	72	454	22.3	19	89
	8	587	489	98	534	28.8	19	115
	7	644	540	104	600	29.3	19	117
	6	744	628	116	686	30.9	19	124
	5	855	771	84	815	20.9	19	84

Method	Location depth	Max (μM)	Min (μM)	Diff. (μM)	Mean (μM)	±σ (μM)	n	Slope dC/dz	Δz (m) estimated
Pipeline [P]	EB-400	1.75	1.35	0.40	1.62	0.10	34	0.0038	105
	KL-430	1.90	1.45	0.45	1.67	0.12	26	0.0038	128
	TF-662	2.44	2.07	0.36	2.33	0.08	34	0.0036	86
Pipeline [Si]	EB-400	47.61	30.84	16.77	38.99	4.55	34	0.150	121
	KL-430	49.37	32.65	16.72	39.95	4.63	26	0.150	123
	TF-660	91.62	67.07	24.55	82.43	5.17	34	0.175	118
Shipboard [P]	ORI-400	1.70	1.50	0.20	1.60	0.07	11	0.0038	76
	ORI-600	2.30	2.10	0.20	2.22	0.08	11	0.0036	89
Shipboard [Si]	ORI-400	48.83	35.05	13.79	40.38	4.09	11	0.150	109
	ORI-600	82.39	66.16	16.23	74.24	5.16	11	0.170	122

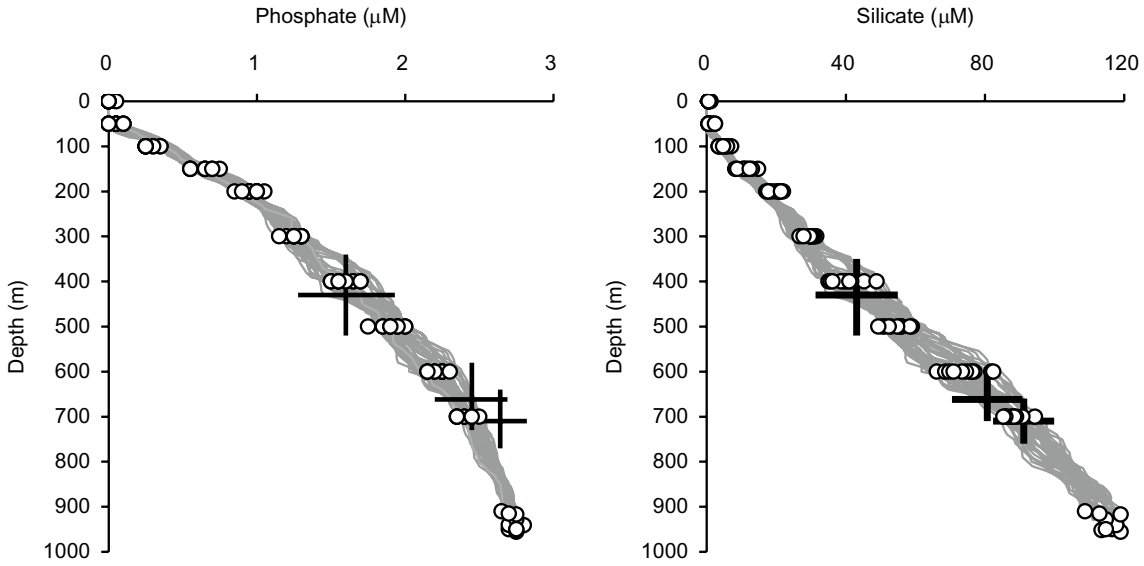

Fig. 8 Composite profiles for (*left*) phosphate and (*right*) silicate at the anchored station 4 km off Hualien coast between Nov 4 and 5. (*Circles*) Discrete data measured for 11 rosette sampling casts. (*Lines*) Continuous nutrient profiles $C_P(1/T)$ and $C_{Si}(1/T)$ are based on temperature data of 19 CTD casts at the same site following Eq. (6) in Sect. 3.4.6. (*Crosses*) Verdicts of maximum vertical displacements by taking account of $\pm 2\sigma$ of P or Si concentrations from Table 2 and Fig. 3, then calculated by Eq. (2)

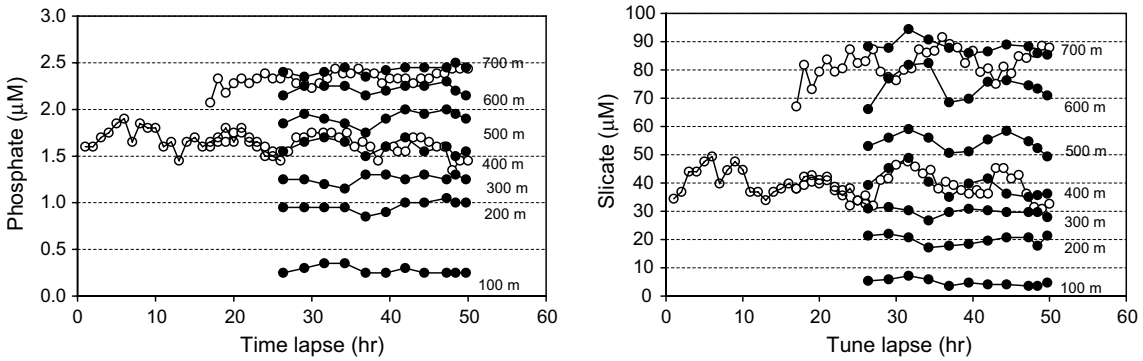

Fig. 9 (*Dots*) Temporal variations of nutrients (*left* phosphate; *right* silicate) of shipboard data at different sampling depths. (*Circles*) Variations in nutrients in pipeline water of KL-430, EB-400, and TF662 taken from Fig. 4

the surface tide. On the other hand, the data for the TF-662 pipeline is obviously 2 h adrift the surface tide. The phase difference between KL-430/EB-400 and TF-662 is approximately 4 h. The relative phase lag is explained by the extra travel time in the pipeline. According to Table 1 the travel times in pipelines are normally 0.9 h for KL-430, 1.3 h for EB-400, and 2.2 h for TF-662. However, according to the operation log sheet of TF-662, the pumping rate was only ca. 40% of the maximum on that day (1000 instead of 2400 ton day^{-1}). Therefore, it might take a longer travel time of 5.3 h to deliver the water from the intake point to the sampling location. The extra travel time was $5.3 - 1.3 = 4$ h. In Fig. 10c, if the TF-662 curve is shifted 4 h to the left, it does synchronize perfectly well with the EB-400 curve. In Fig. 10d, the TF-662 curve is also off-phased with the shipboard data (ORI-600 and ORI-700). Again, by shifting the TF-662 curve 4 h to the left, in Fig. 10e, the phase lag is likely diminished. Theoretically, the EB-400 curve should lead the ORI-400 curves by 1.3 h. However, the two data sets plotted in Fig. 9 are too scattered to identify such a small difference.

3.4.6 Relationship between nutrients and temperature

In an earlier work the relationship between nutrient concentration and temperature of a specific ocean area was presented as an empirical polynomial equation (Pai et al. 2015):

$$C(T)(\mu\mathrm{M}) = a_0 + a_1 T + a_2 T^2 + \cdots + a_n T^n \tag{5}$$

where a_0 … a_n are empirical constants and n the power order. However, there are two drawbacks when using this high-order equation. First, the T^n term value increases as n increases, so the significant figures of the a_n term must be extended to larger decimals. Second, the inverse calculation from C to T would be difficult. For these reasons, an exponential approach has been adopted here in which the concentration C is implemented as a function of $1/T$ (Fig. 11):

$$C(1/T)(\mu\mathrm{M}) = C_0 + C_\mathrm{m}[1 - \exp(-k(1/T - a))]^n 4^\circ\mathrm{C} < T < 25^\circ\mathrm{C} \tag{6}$$

where $1/T$ is the reciprocal of temperature in the °C^{-1} units, C_0 is the concentration (μM) in the surface mixing layer, C_m a hypothetical maximum concentration along the water column, k and n are empirical constants, and a is the reciprocal value of 25 °C. Empirical fittings with simple values gave satisfactory results: For phosphate, $C_0 = 0$, $C_\mathrm{m} = 2.9$, $k = 15.5$, $a = 0.04$, $n = 1.2$, whereas for silicate, $C_0 = 1$, $C_\mathrm{m} = 147$, $k = 10.5$, $a = 0.04$, $n = 1.7$. Composite profiles for phosphate and silicate are presented in Fig. 8. The lines were generated by the above equation according to the temperature data of 19 CTD down-casts.

Inversely, temperature T can be readily estimated from measured concentration C by the following calculation:

$$T(^\circ C) = 1/\left[a - \frac{1}{k}\ln\left(1 - \left(\frac{C - C_0}{C_\mathrm{m}}\right)^{\frac{1}{n}}\right)\right] (C_0 < C < C_\mathrm{m}) \tag{7}$$

The demonstrate the usage of Eq. (7), data taken from Fig. 4 were used to calculate for the intake temperature and the results are plotted in Fig. 12. Results obtained by phosphate concentration coincide well with that by silicate concentration. For the KL-400 pipeline, the max. and min. temperatures are 8.8 and 11.2 °C, with a daily variation range of 2.4 °C. For the EB-400 pipeline, the range is 9.3–11.6 °C, whereas 5.6–8.0 °C for the TF-662 pipeline. These results clearly indicate that a daily variation of ca. 2.4 °C will be expected to occur at the pipeline intake

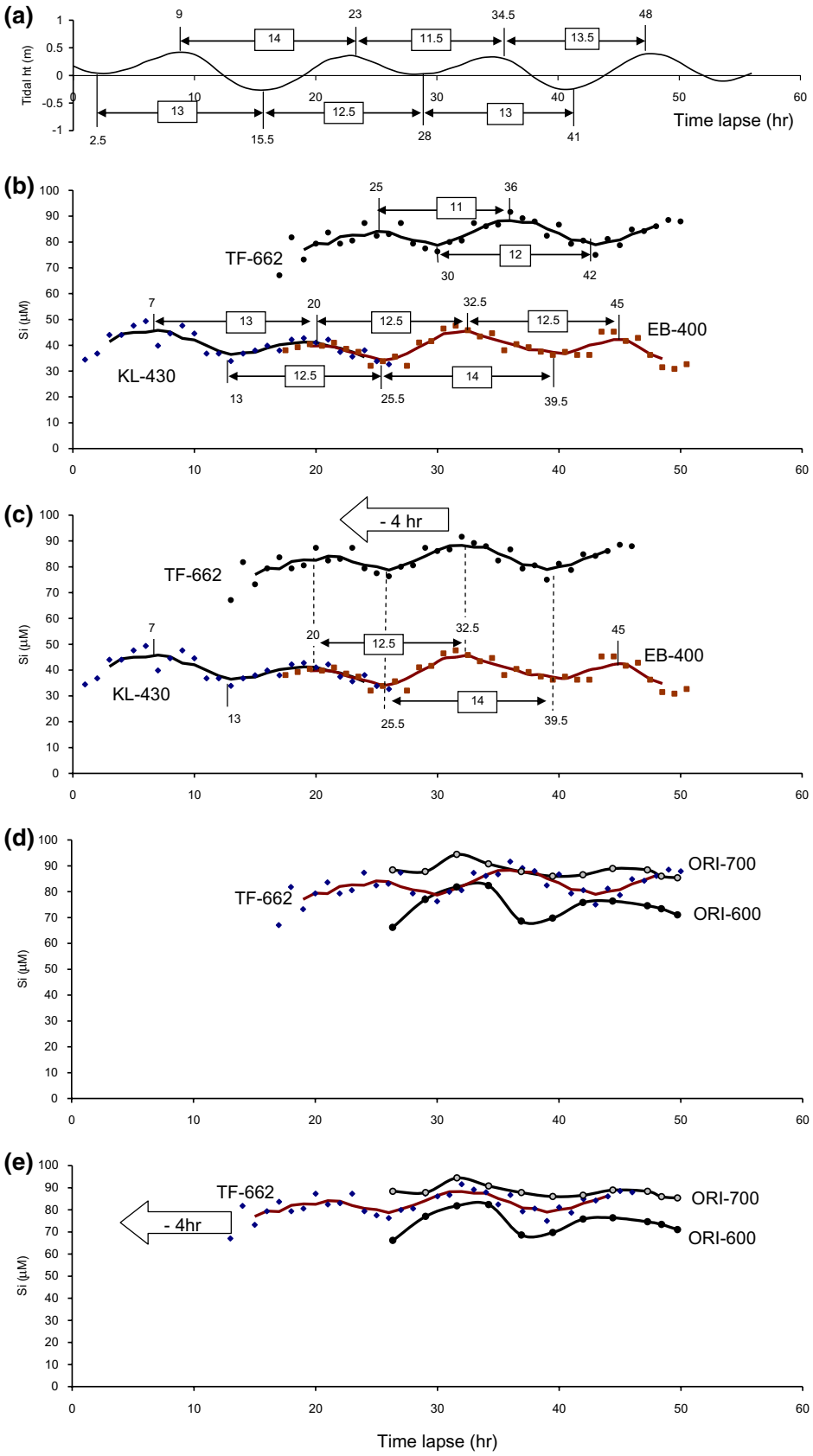

Fig. 10 A moving average process of discrete Si data sets reveals that semidiurnal cycles exist in the pipeline water. **a** The surface tidal record (starting from 15:00 pm, Nov 3, 2015) indicating a typical semidiurnal tide. **b** Silicate concentration variations in pipelines KL-430/EB-400 also show semidiurnal cycles, but the phase is likely 2 h ahead of the surface tide. The data for the TF-662 pipeline is likely 2 h adrift the surface tide. **c** The phase lag between KL-430/EB-400 and TF-662 can be adjusted by shifting the latter *curve* 4 h ahead so they look synchronized. The 4 h is accounted for the extra delay time in the TF-662 pipeline. **d** The off-phase is obvious between the TF-662 *curve* and shipboard *curves* at 600 and 700 m depth, respectively. **e** By shifting the TF-662 *curve* 4 h to the *left* the phase lag is likely diminished

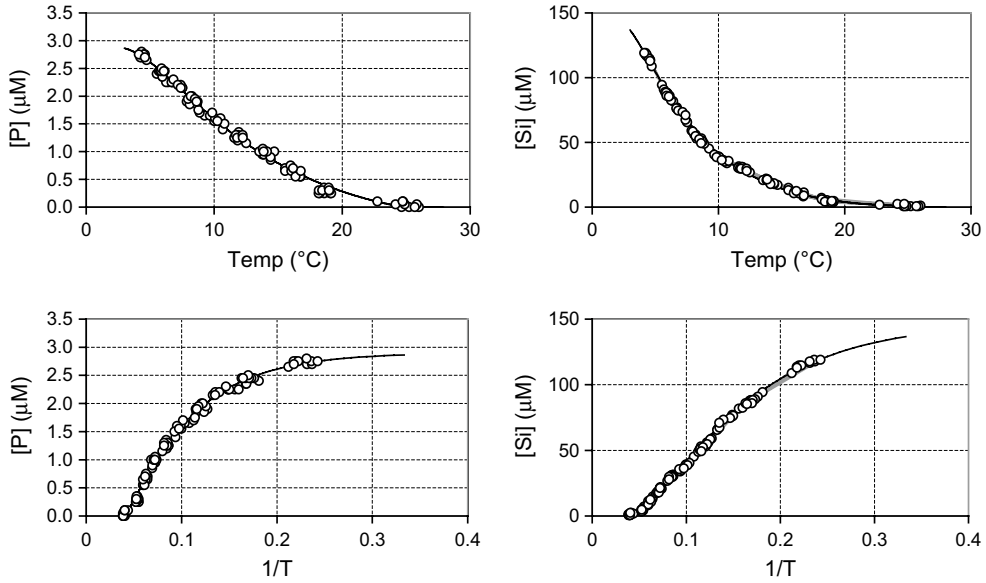

Fig. 11 Relationships between nutrient concentrations and temperature (T and $1/T$) along the water column off Hualien coast. Circles are measured nutrient data at different depths in 11 up-casts with corresponding CTD down-cast temperature data. The relationship can be expressed by an empirical polynomial equation, but in this study an empirical exponential equation C = function $(1/T)$ is highly recommended

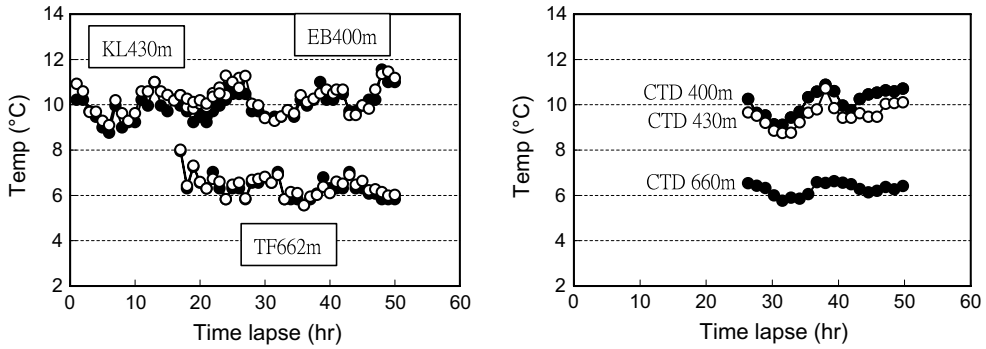

Fig. 12 (*Left*) Phosphate and silicate data taken from Fig. 4 were used to calculate for the intake temperature using Eq. (7). The results from phosphate (*dot*) and silicate (*circle*) coincide with each other perfectly. (*Right*) In situ temperature measured directly by CTD at 400, 430, and 660 m, respectively

points, matching perfectly with the direct measurements by the CTD sensor (also in Fig. 12). It explains why the water temperature as observed at each pumping station is always changing in an up and down manner within a day and how it is connected to the internal tides.

3.4.7 [Si]/[P] ratio

Although both silicate and phosphate concentrations are low in the surface layer and increase with depth to give "nutrient-type" distributions, they are not parallel. In this study, the relationship between [Si] and [P] can be described by an empirical curve (Fig. 13):

$$[\mathrm{Si}]\,(\mu\mathrm{M}) = 3.6027[\mathrm{P}]^3 - 0.5549[\mathrm{P}]^2 + 16.342[\mathrm{P}] + 1 \quad 0 < [\mathrm{P}] < 2.8 \tag{8}$$

The [Si]/[P] ratio (or slope) increases with depth and concentrations. For surface layer or [P] < 1 μM, the [Si]/[P] ratio is ca. 20. The ratio increases to ca. 30 at [P] = 2.0 μM, and to ca. 38 at [P] = 2.5 μM.

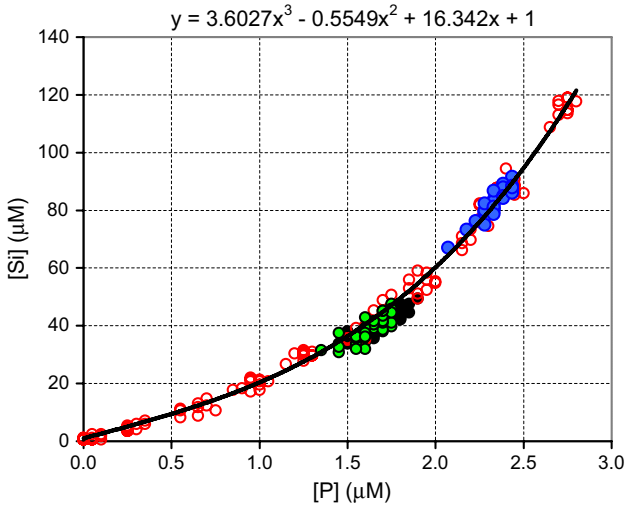

Fig. 13 Relationship between silicate and phosphate in the Hualien area. Data points include all pumping station data (*dots*) as well as off-shore water column data from R/V Ocean Researcher I (*circles*). The [Si]/[P] ratio is 20 at low concentration level ([P] < 1.0 μM), gradually increases to 30 at [P] = 2.0 μM and to nearly 38 at [P] = 2.5 μM level

Although either nutrient can be used to estimate temperature, we recommend that both parameters are to be monitored as a double check to ensure data quality.

4 Conclusion

Routine monitoring of dissolved phosphate and silicate in pipeline seawaters (taken from 400 to 710 m layers off the Hualien coast) has shown regular concentrations changes. Through an intensive "land-sea" monitoring experiment this phenomenon has been confirmed to be the result of semidiurnal internal tides occurring in almost the entire water column (from 50 m down to the bottom at 950 m). The maximum vertical displacements can reach to nearly 100 m in the intermediate layer between 300 and 800 m or 12–5 °C. The ship-obtained nutrient data showed consistent correlations with temperature, which has been used to construct empirical exponential equations for the water column off the Hualien coast. The measurement of nutrients in pipeline water gives an indication of the vertical oscillation of the water mass at the 400–700 m layer. The pipelines also serve as chemical sensors which enable oceanographers to monitor the composition of the deep-layer seawater continuously for further scientific investigation.

Acknowledgements The project was sponsored by the Taiwan Society of Deep Ocean Water Resources Application (TW-SOWA). The field work could not have been accomplished without help from many volunteer participants including students on their internship cruise. The captain and crew of R/V Ocean Researcher 1, and the staff at three factories as listed in Table 1 are all deeply appreciated. SCP and SJ were also sponsored by the Ministry of Science and Technology (Taiwan) under grant no. 104-2611-M-002-018 and 104-2611-M-002-010. The authors would also like to express their gratitude to three anonymous reviewers for their kind and useful criticism of the manuscript. This paper is dedicated to WHL, the senior technician, who died in line of duty during Cruise ORI-1158 on Feb 22, 2017.

References

Alford MH, MacKinnon JA, Nash JD, Simmons H, Pickering A, Klymak JY, Pinkel R, Sun O, Rainville L, Musgrace R, Beitzel T, Fu KH, Lu CW (2011) Energy flux and dissipation in Luzon Strait: two tales of two ridges. J Phys Oceanogr 41(11):2211–2222. doi:10.1175/JPO-D-11-073.1

Alford MH, Peacock T, MacKinnon JA, Nash JD, Buijsman MC, Centuroni LR, Chao SY, Chang MH, Farmer DM, Fringer OB, Fu KH, Gallacher PC, Graber HC, Helfrich KR, Jachec SM, Jackson CR, Klymak JM, Ko DS, Jan S, Johnston TMS, Legg S, Lee IH, Lien RC, Mercier MJ, Moum JN, Musgrave R, Park JH, Pickering AI, Pinke R, Rainville L, Ramp SR, Rudnick DL, Sarkar S, Scotti A, Simmons HL, St Laurent LC, Venayagamoorthy SK, Wang YH, Wang J, Yang YJ, Paluszkiewicz T, Tang TY (2015) The formation and fate of internal waves in the South China Sea. Nature 521:65–69. doi:10.1038/nature14399

Chen CTA (2005) Tracing tropical and intermediate waters from the South China Sea to the Okinawa Trough and beyond. J Geophys Res 110(C5):C05012. doi:10.1029/2004JC002494

Jan S, Chern CS, Wang J, Chao SY (2007) Generation of diurnal K1 internal tide in the Luzon Strait and its influence on surface tide in the South China Sea. J Geophys Res 112(C6):C06019. doi:10.1029/2006JC004003

Jan S, Lien R, Ting C (2008) Numerical study of baroclinic tides in Luzon Strait. J Oceanogr 64(10):789–802. doi:10.1007/s10872-008-0066-5

Jan S, Yang YJ, Wang J, Mensah V, Kuo TH, Chiou MD, Chern CS, Chang MH, Chien H (2015) Large variability of the Kuroshio at 23.75°N east of Taiwan. J Geophys Res 120(C3):1825–1840. doi:10.1002/2014JC010614

Lien RC, Tang TY, Chang MH, D'Asaro EA (2005) Energy of nonlinear internal waves in the South China Sea. Geophys Res Lett 32(5):L05615. doi:10.1029/2004GL02212

Lien RC, Sanford TB, Jan S, Chang MH, Ma BB (2013) Internal tides on the East China Sea continental slope. J Mar Res 71(1–2):151–185. doi:10.1357/002224013807343461

Lien RC, Henyey F, Ma B, Yang YJ (2014) Large-amplitude internal solitary waves observed in the northern South China Sea: properties and energetics. J Phys Oceanogr 44(4):1095–1115. doi:10.1175/JPO-D-13-088.1

Mensah V, Jan S, Chiou MD, Kuo TH, Lien RC (2014) Evolution of the Kuroshio Tropical Water from the Luzon Strait to the east of Taiwan. Deep-Sea Res I 86(4):68–81. doi:10.1016/j.dsr.2014.01.005

Mensah V, Jan S, Chang MH, Yang YJ (2015) Intraseasonal to seasonal variability of the intermediate waters along the Kuroshio path east of Taiwan. J Geophys Res 120(C8):5473–5489. doi:10.1002/C010768

Niwa Y, Hibiya T (2004) Three-dimensional numerical simulation of M2 internal tides in the East China Sea. J Geophys Res 109(C4):C04027. doi:10.1029/2003JC001923

Pai SC, Yang CC, Riley JP (1990) Effects of acidity and molybdate concentration on the kinetics of the formation of the

phosphoantimonylmolybdenum blue complex. Anal Chim Acta 229:115–120. doi:10.1016/S0003-2670(00)85116-8

Pai SC, Jan S, Chu KS, Huang PY, Takahashi MM (2015) Kuroshio or Oyashio—sources of the 700 m deep ocean water off Hualien coast, eastern Taiwan. Deep Ocean Water Res 15(3):107–116. http://www.dowas.net/english/journals/15-3.html

Takahashi MM, Huang PY, Lee SC (2012) Current status of deep ocean water resource utilization in Taiwan. Deep Ocean Water Res 13:41–52. http://www.dowas.net/paper/13-1.html **(in Japanese with English abstract)**

Ting CH (2009) Design of a new-type flow analysis for the simultaneous determination of silicate and phosphate and its application to ocean environmental studies. M.Sc. thesis, Institute of Oceanography, National Taiwan University, pp 65 **(in Chinese with English abstract)**